Nano Energy (2015) 16, 28–37

Available online at www.sciencedirect.com

ScienceDirect

journal homepage: www.elsevier.com/locate/nanoenergy

RAPID COMMUNICATION

Investigation of surface effects through the application of the functional binders in lithium sulfur batteries

Guo Ai[a,b], Yiling Dai[a], Yifan Ye[c,d], Wenfeng Mao[a], Zhihui Wang[a], Hui Zhao[a], Yulin Chen[a], Junfa Zhu[d], Yanbao Fu[a], Vincent Battaglia[a], Jinghua Guo[c], Venkat Srinivasan[a], Gao Liu[a,*]

[a]*Energy Storage and Distributed Resources Division, Energy Technologies Area, Lawrence Berkeley National Laboratory, Berkeley, CA 94720, United States*
[b]*Science and Technology on Reliability Physics and Application of Electronic Component Laboratory, No. 5 Electronic Research Institute of the Ministry of Industry and Information Technology, Guangzhou 510610, China*
[c]*Advanced Light Source, Lawrence Berkeley National Laboratory, Berkeley, CA 94720, United States*
[d]*National Synchrotron Radiation Laboratory and Collaborative Innovation Center of Suzhou Nano Science and Technology, University of Science and Technology of China, Hefei, Anhui 230029, China*

Received 14 March 2015; received in revised form 27 May 2015; accepted 31 May 2015
Available online 11 June 2015

KEYWORDS
Li–S batteries;
Conductive binder;
Surface effect;
Self-discharge;
Binding energy;
Cell failure

Abstract
Sulfur species dissolution, precipitation and phase transformation during the charge and discharge process strongly affect the performance of lithium sulfur (Li–S) batteries. Interface properties between electrode and electrolyte play an important role in these batteries. In this work, four kinds of binders with different functionalities, which differs both in chemical and electrical properties, are employed to study how the interface properties affect the battery reaction mechanism. The phase transformation of sulfur species is studied in detail. Remarkable differences are observed among sulfur cathodes with different binders. More solid-phase sulfur species precipitation is observed with binders that have carbonyl functional groups, like poly(9, 9-dioctylfluorene-co-fluorenone-co-methylbenzoic ester) (PFM) and poly(vinylpyrrolidone) (PVP), in both fully charged and discharged states. Also, the improved conductivity from introducing conductive binders greatly promotes sulfur species precipitation. These findings suggest that the contributions from functional groups affinity and binder conductivity lead to

*Corresponding author at: Energy Storage and Distributed Resources Division, Energy Technologies Area, Lawrence Berkeley National Laboratory, Berkeley, California 94720, United States. Tel.: +1 510 486 7207; fax: +1 510 486 7303.
E-mail address: gliu@lbl.gov (G. Liu).

http://dx.doi.org/10.1016/j.nanoen.2015.05.036
2211-2855/Published by Elsevier Ltd.

more sulfur transformation into the solid phase, so the shuttle effect can be greatly reduced, and a better cell performance can be obtained.
Published by Elsevier Ltd.

Introduction

Li–S batteries have attracted a great amount of attention due to their high theoretical gravimetric specific capacity, low cost, and environmental benignity [1–5]. However, they also have a few shortcomings, such as relatively poor cycling life, low coulombic efficiency, and high self-discharge loss [6], which have hindered their practical application. These limitations mainly result from the low conductivity of the solid products (S_8 and Li_2S) [5,7] and the shuttle effect of the dissolved lithium polysulfide in the electrolyte [8–10]. It is well known that Li–S batteries are noted for phase transformation during cycling. In a Li–S cathode composed of non-encapsulated sulfur particles, conductive additive (acetylene black, AB), and polymer binder, the sulfur dissolves as polysulfide and precipitates as sulfur or lithium sulfide during cycling. In discharge processes, solid-phase S_8 dissolves into soluble Li_2S_x (x=2–8) and then precipitates to solid-phase Li_2S. Correspondingly, in charge processes, Li_2S gradually dissolves into soluble polysulfide and then may return to solid-phase S_8 or long-chain polysulfide Li_2S_8 [11]. During both charge and discharge processes, the electrode provides a conductive matrix for the solid sulfur species to precipitate. The matrix surface chemistry determines the interaction (covalent bonding or physical absorption) between the matrix and the sulfur species, so a strong covalent bonding can help fix sulfur species to the cathode matrix. This fixation can reduce the polysulfide shuttle effect and improve long-term performance stability [12,13]. AB is generally used as conductive additive in the conductive matrix, but research shows that the binding energy between solid sulfur species and AB is very low, and possible detachment of solid sulfur species from AB surface may exist [14]. However, since the particle surface of AB is covered by the polymer binders to form the matrix, the predominate surfaces for sulfur species precipitation are the polymer binders [15,16]. Therefore the functionality of binders has a crucial impact to the performance of Li–S batteries.

The electrochemical performance of batteries is greatly improved through binder design [17–23]. Different kinds of polymer binders have been applied in Li–S batteries. Early works mainly focus on non-conductive polymers as binders, which include poly(vinylidenedifluoride) (PVDF) [24,25], poly (vinylpyrrolidone) (PVP) [15], gelatin [26], styrene–butadiene rubbers (SBR) [27], and others. They mainly act as binding agents to glue the active material and conductive additives together and maintain the integrity of the electrode. Recently, conductive binders have been introduced into Li–S battery system, and a noted improvement in battery performance is obtained [18–20,28]. The conductive binders can act as both the binding agents and the conductive framework in Li–S batteries. The most well-known conductive binder is poly(3,4-ethylenedioxythiophene):polystyrene sulfonate (PEDOT:PSS, written as PEDOT for short in this paper) [18], which is also widely used in photovoltaic and photoelectronic devices. It shows much improved performance over non-conductive binders in Li–S batteries [29]. Still, a detailed understanding of how conductive binders can improve battery performance needs to be investigated.

In this work, four kinds of binders with different functional groups and conductive properties are employed to study how the interface chemical properties and binder conductivity affect the battery reaction mechanism. Poly (9,9-dioctylfluorene-co-fluorenone-co-methylbenzoic ester) (PFM) is specially designed and synthesized in our group [19,20]. It has two carbonyl groups and is highly conductive. Although originally designed for Si electrode, PFM also has a high binding energy with sulfur species (Li_2S_x, x=1–8) through incorporation of the fluorenone carbonyl (C=O) group and methylbenzoic ester-$PhCOOCH_3$ (MB) group [15] and shows superior performance in Li–S batteries. Thus, PFM is selected to illustrate the importance of both the functional groups and the conductive properties of binders on battery performance. The second binder introduced in this work is a well-known conductive binder, PEDOT:PSS water dispersion. Between PFM and PEDOT, we compare the influence of functional groups on the cell reaction mechanism when both binders are conductive. The third binder introduced is a non-conductive binder, PVP, which has amide carbonyl functional groups and a high binding energy with Li_2S_x (x=1–8) [15]. By comparing the performance between PFM and PVP, we demonstrate how the binder's electronic conductivity can improve the performance of the cell when they both have carbonyl groups to bind with sulfur species on the conductive matrix. Also, PVDF, the most commonly used non-conductive binder for both lithium-ion and Li–S batteries, is studied for comparison. By comparing the difference in morphology and structure of sulfur species after cycling, our work suggests that the functional binders have a major influence on battery performance through surface functionality on the electrode. With the assistance of the carbonyl group and high conductivity of the binder, more solid products (S_8 in charged state and Li_2S in discharged state) are observed and a suppression of polysulfide dissolution is obtained. This provides us a new direction of electrode design to further improve Li–S battery performance.

Material and methods

Materials

The micrometric sulfur powder is purchased from Mallinckrodt Company, and acetylene black (AB) is purchased from Denka Japan. Four binders are used in this work, and PFM is synthesized according to previous work [19]. The PEDOT and PVP are purchased from Sigma-Aldrich Inc. The PVDF is purchased from Kureha America, Inc. The N-methyl-2-

pyrrolidone (NMP) (anhydrous, 99.5%) is purchased from Sigma-Aldrich Inc. and used as the solvent for the laminate with PVP and PVDF as binders. The chlorobenzene (Sigma-Aldrich Inc.) is used as the solvent for PFM. The electrolyte for cell testing is composed of 1 M lithium salt bis(trifluoromethanesulfonyl)imide (LiTFSI) dissolved in polyethylene glycol dimethyl ether (PEGDME) and 1 wt% $LiNO_3$, all purchased from Sigma-Aldrich. The molecular weight of the PEGDME is around 500 Da.

Cathode fabrication

The PVP and PVDF are first dissolved in NMP, while PFM is dissolved in chlorobenzene, and PEDOT is diluted by deionized water, all at 5 wt% ratio. Commercial micrometric sulfur powder and AB are added into the binder-solvent solution after the binder is dissolved. The weight ratio of these three components is: 50% sulfur, 10% binder, and 40% AB. The mixture is mixed by a ball-milling method overnight to obtain uniform slurry. The laminate is then made by coating the slurry on an 18-μm-thick battery-grade aluminum current collector with a Mitutoyo doctor blade and an Elcometer motorized film applicator. Typical mass loading of sulfur is 0.3 mg/cm^2. After the laminate is fully dried, it is further dried in a vacuum oven at 50 °C overnight.

Cell assembly and testing

Li–S batteries are tested with 2325-type coin cells (National Research Council Canada). The cells are assembled in an argon-filled glove box with oxygen content less than 0.1 ppm. The size of the sulfur electrode is 1/2-in. OD, and the size of the counter-electrode lithium metal disk is 11/16-in. OD. The Li foil is purchased from FMC-Lithium Co. The separator used is polypropylene film (Celgar 2400). Galvanostatic cycling tests are performed on a Maccor series 4000 cell tester (Maccor, Inc., Tulsa, OK). The voltage window for cell test is 1.5–2.6 V. The cells are cycled at C/10 for 10 cycles to get a relatively stable performance. After the first 10 cycles, the self-discharge test is performed by charging the cells to the fully charged state and then letting them rest for 60 h. This procedure is repeated three times, with the third rest lasting 240 h. With this cycling procedure, both the cycling performance for the cathodes and the self-discharge prevention ability can be obtained.

Material characterization techniques

Morphology of the electrode surface is characterized with a JSM-7500F scanning electron microscope at the National Center for Electron Microscopy (NCEM) at Lawrence Berkeley National Laboratory. The cycled Li–S batteries are opened with a cell opener, and the electrode is washed thoroughly with 1,3-dioxolane/1,2-dimethoxyethane (DOL/DME) with a volume ratio of 1:1 inside an argon-filled glove box.

For the total fluorescence yield near-edge X-ray absorption fine structure (TFY-NEXAFS) experiments, the cells are disassembled in fully discharged state after cycling for 50 cycles and washed with DOL/DME 1:1 solution thoroughly in the glove box. The samples are peeled off from the current collector and well-sealed using 2.53 μm-thick Kapton film. The S K-edge X-ray absorption spectra are collected at beam line 9.3.1, 10.3.2 at Lawrence Berkeley National Laboratory's Advanced Light Source. This is a bending magnet beam line with photon energies ranging from 2320 to 5600 eV (9.3.1) and 2400 to 17,000 eV (10.3.2) and an unfocused beam size of 1 mm∗0.7 mm (9.3.1) and 20 μm∗16 μm (10.3.2). Total fluorescence signals are collected with a channeltron with an approximately 0.36 eV resolution. The photon incident angle is set at 45° for all samples. Probing depth of up to a few microns can be achieved.

Results and discussion

Cycling and self-discharge performance of cathodes with different binders

In this work, four binders are introduced to study the surface effect in Li–S battery working mechanism. PFM and PEDOT are conductive binders, while PVP and PVDF are non-conductive binders. The chemical structures of these four binders are shown in Figure 1a. PFM and PVP both have carbonyl groups, while PEDOT and PVDF do not. The four cathodes with PFM, PEDOT, PVP and PVDF are named PFM-S, PEDOT-S, PVP-S and PVDF-S for short. The cycling test is designed by regular cycling procedures with three self-discharge tests as intervals. The 60 h, 60 h, and 240 h self-discharge tests are set after the tenth, twentieth, and thirtieth cycles. The procedure tests both the cycling performance and the self-discharge prevention ability for four cathodes with different binders. As shown in Figure 1b, four cathodes show almost the same specific capacity at the first few cycles, but the PFM-S shows the smallest decay in the following cycling test. With the help of the good conductivity, the PEDOT-S shows a good performance, but the capacity decay is larger than that of PFM-S. Among all cathodes, the PVP-S shows the smallest specific capacity in the first few cycles, probably due to the incomplete reduction of sulfur wrapped by the non-conductive binder PVP at the beginning. The performance of PVP-S is better than that of PEDOT-S and inferior to that of PFM-S, indicating that both the high conductivity and the functional group of the binder are important to achieve high performance in the Li–S batteries.

The self-discharge evaluation highly depends on the cells status, so we test all the cells in the full charged state to be a fair comparison [6]. The change of open circuit voltage during rest in Figure 1c is one of the most straightforward ways to show the self-discharge prevention ability of different cathodes. The open circuit voltage is closely related to the resultant sulfur species in fully charged state and their reaction activity. During both the 60-h and the 240-h rest, PFM-S shows almost no voltage drop, while the other three cells (PEDOT-S, PVP-S, and PVDF-S) show clear voltage drops. This open circuit voltage drop in the three types of cells is a clear indication of a significant conversion of sulfur or long chain polysulfide into shorter polysulfide through the self-discharge process [6]. The dissolved polysulfide molecular diffuses to the anode side, reacts with the Li metal and forms shorter chain polysulfide. The open circuit voltage drop highly relates to how much polysulfide

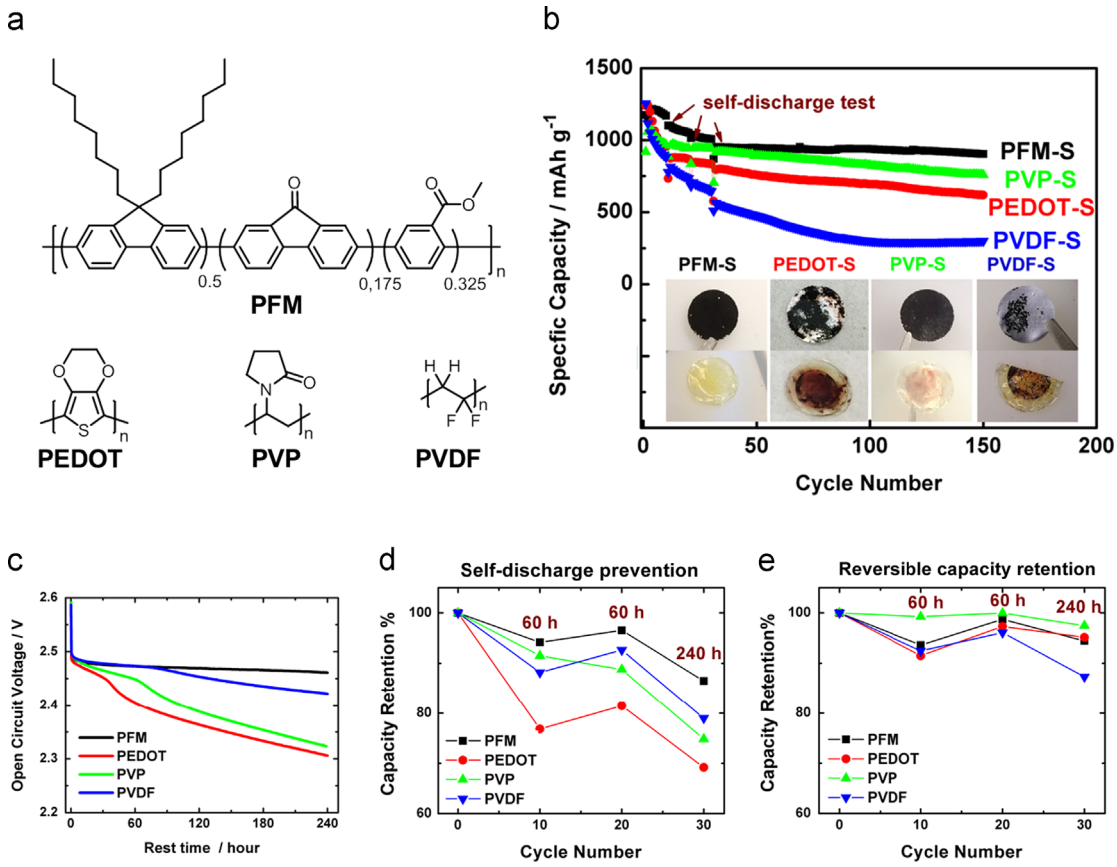

Figure 1 (a) Chemical structures of the four different binders: PFM, PEDOT, PVP, and PVDF. (b) Cycling performance at C/10 and self-discharge performance of cathodes with different binders. (c) The open circuit voltage change vs. rest time during the third self-discharge rest of 240 h for the PFM-S, PEDOT-S, PVP-S, and PVDF-S cathodes. The self-discharge capacity prevention ratio (d) and reversible capacity retention ratio (e) for cathodes with different binders during the self-discharge test.

is dissolved in the electrolyte, and its rate of reduction at the Li metal side. The open circuit voltage stability of PFM-S indicates the majority of sulfur species is attracted by the functionalities on the binder and less free polysulfide is dissolved in the electrolyte. So, with the help of the surface modification effect of binders, difference exists in sulfur species reaction mechanism of different cathodes.

The self-discharge prevention ability of cathode can also be characterized by two other factors. One is the self-discharge prevention factor Q_{sd}, which shows the capability of the cell to prevent its capacity loss during the rest in its fully charged state

$$Q_{sd} = \frac{C_a}{C_b}$$

C_a is the immediate discharge capacity after rest; C_b is the discharge capacity before rest.

The other factor is the reversible capacity retention factor Q_r, which shows the ratio of capacity that could be recovered after self-discharge rest

$$Q_r = \frac{C_f}{C_b}$$

C_f is the discharge capacity of the following cycle after rest; C_b is the discharge capacity before rest. The self-discharge performance is plotted in Figure 1d and e. The self-discharge prevention factor in Figure 1d is plotted by the residual capacity ratio immediately after each rest period. The reversible capacity retention factor Q_r in Figure 1e is plotted by the reversible capacity ratio in the following cycle after rest. The capacity loss from cycling is not included in these two factors.

We note that in most cases, the self-discharge capacity prevention factor Q_{sd} for each cathode decreases with longer rest times. Also, the capacity loss for the second 60-h test is less than the first 60-h test. This is because the side reaction is reduced after more cycles and a more stable performance is obtained. In all three self-discharge test, the PFM-S and PVP-S show better self-discharge capacity prevention factor Q_{sd}, and reversible capacity retention factor Q_r than the other two. This is because in the cathodes with functionalized binders (PFM and PVP), the majority of sulfur species are attracted by the functionalities on the binder and less free polysulfide is dissolved in the electrolyte. They are efficient in keeping the active sulfur species from self-discharge in fully charged state, which is consistent with the conclusion deduced from the open circuit voltage profile results. But the surface functionalities on the PFM are connected to the conductive network, so the functional groups are very effective in retaining sulfur species. Although the similar functional group is on PVP, because the polymer is not conductive, the functional group

on PVP is not very effective in assisting the deposition of sulfur species. This affords the best capacity retention of PFM-S. For PVDF-S, since the capacity loss is more severe than the other three, it will lead to fewer amounts of sulfur species in the cell and a thicker passivation film on lithium electrode, which prevents the fast reaction between dissolved sulfur species and lithium electrode. Therefore, a smaller open circuit voltage drop is observed for PVDF-S than PEDOT-S and PVP-S, although the former one's performance is worse than later two. In all, we can conclude that the binding to sulfur species provided by the functional groups on the PFM and PVP binders provides better sulfur species retention in the electrode. Therefore, they can afford much better self-discharge prevention and capacity retention ability in both PFM-S and PVP-S electrode.

Morphology of cathodes with different binders in charged and discharged state

All four types of electrodes are made of same amount of sulfur and AB, but vary the binder type only. The binders cover the surface of the AB to form a continuous conductive matrix for the electrodes, providing a functioned surface to interact with sulfur species. To study the mechanism of the surface functional group effect of different binders on cycling performance, the cells are disassembled both in fully charged and discharged states, and the cathodes are thoroughly washed for morphology study. As shown in Figures 2 and 3, differences in morphology can be observed in these electrodes, both in the charged state and the discharged state, indicating different amounts of solid sulfur species precipitation [11,30]. It should be point out that more solid product precipitation is observed for PFM-S, both in the charged and discharged states. In addition, the cathodes with conductive binders exhibit more uniform precipitation morphologies than those with non-conductive ones. This suggests that functionality of the binders has major influence on solid-phase sulfur species precipitation.

When the cells are disassembled in the fully charged state, both the electrode integrity and the appearance are different for cathodes with different binders, as shown in Figure S1. During the cell disassembly and washing process, no delamination is observed in the electrode of the PFM-S (Figure S1a), and almost none of the reddish color electrolyte, which is the typical color for polysulfide, can be seen in the opened cell (Figure S1e). This indicates that in the fully charged state, with the functionality of the PFM binder, the sulfur species can be precipitated on the electrode matrix, helping the PFM-S electrode to maintain its integrity. The integrity of PVP-S is good (Figure S1c), but the PEDOT-S partially delaminates from the current collector (Figure S1b), and the PVDF-S fragments into small pieces (Figure S1d). Correspondingly, a light reddish color electrolyte can be observed for PVP-S (Figure S1g), while a deeper red electrolyte is observed for the PEDOT-S and PVDF-S (Figure S1f and S1h). The deeper red color in electrolyte corresponds to the color of long chain polysulfide. The sulfur species remains dissolved in electrolyte as long-chain deep red polysulfide (Li_2S_8 or Li_2S_6), instead of precipitating as solid-phase sulfur, for PEDOT-S and PVDF-S in the fully charged state. The dissolved phase of polysulfide results in a more severe shuttle effect during cell operation, which negatively impacts the cell performance.

The morphology of four cathodes with different binders is observed by SEM in fully charged state in Figure 2. A layer of solid-phase substance is clearly observed coating the AB particle surface in PFM-S and PVP-S (Figure 2a and c), which is identified as the precipitated sulfur species by EDX. In comparison, for PEDOT-S and PVDF-S, almost none of this solid phase precipitation substance is observed (Figure 2b and d). This further supports the earlier suggestion that in the fully charged state, the sulfur species precipitates as solid-phase sulfur in PFM-S and PVP-S, while in PEDOT-S and PVDF-S the sulfur species remains dissolved in electrolyte as long-chain polysulfide, which has a deep red color (Figure S1f and S1h). To further observe the solid-phase sulfur precipitation, the electrode laminate layer is peeled off from the current collector and observed from the bottom surface (attached to the current collector). For PFM-S, a large amount of solid-phase precipitation can be observed at the bottom (Figure 2e); as much as on the surface (Figure 2a). Uniform sulfur precipitation throughout the film in PFM-S electrode is achieved both by the functional carbonyl group and the conductivity of the binder. For PVP-S, solid-phase sulfur precipitation is observed on the surface (Figure 2c) as in PFM-S, but almost none is observed at the bottom (Figure 2g). The precipitated sulfur on the top surface seems to clog the pores and prevent the polysulfide from penetrating, which leads to insufficient sulfur precipitation near the bottom. So some polysulfide residues are observed in the electrolyte (Figure S1g). This preferential deposition of sulfur species on the top of the electrode is a result of non-uniform conductivity of the electrode caused by the non-conductive binder. This further demonstrates the importance of binder conductivity in sulfur precipitation. In PFM-S, with a much larger conductive surface area for reaction and the assistance of the carbonyl group to fix sulfur, a more uniform sulfur precipitation takes place, and less polysulfide is left in the electrolyte. However, for PEDOT-S (Figure 2b and f) and PVDF-S (Figure 2d and h), no solid-phase precipitation is observed both at the electrode surface and the bottom on AB. This indicates that the carbonyl group is crucial for assisting solid-phase sulfur precipitation in the charged state. In addition, the relative ratio of sulfur to carbon analyzed from EDX data can be used as a proof of sulfur existence. For PFM-S, the ratio of sulfur to carbon is 0.23, while a sulfur-to-carbon ratio of almost zero is observed in PEDOT-S and PVDF-S. The PVP-S only shows subtly more sulfur than PEDOT-S and PVDF-S. The preliminary analysis of the sulfur species is also analyzed with Near-Edge X-ray Absorption Fine Structure (NEXAFS) as Supporting information shown in Figure S2.

With the above observation, the self-discharge prevention ability for different cathodes can be explained. The reactant tends to react spontaneously into lower energy products during the self-discharge test, and this process is greatly slowed down when the reactant is in solid phase. In the PFM-S cathodes, most of the sulfur species is precipitated as solid phase in fully charged state, which can result in good self-discharge prevention ability and no open-circuit voltage drop during long rests. For PVP-S, the open-circuit voltage drop and minor self-discharge loss might come from the very

small amount of residual polysulfide in the electrolyte. And the good reversible capacity retention ability in PVP-S comes from that the binding between amide carbonyl functional group and sulfur species is partially enhanced by the increased polarization in the presence of nitrogen. However, in PEDOT-S and PVDF-S, the sulfur species mainly dissolves in electrolyte as long-chain polysulfide, which tends to react spontaneously and can lead to open-circuit voltage drop. Thus, a much larger self-discharge loss is observed in the cathodes when no carbonyl group is present.

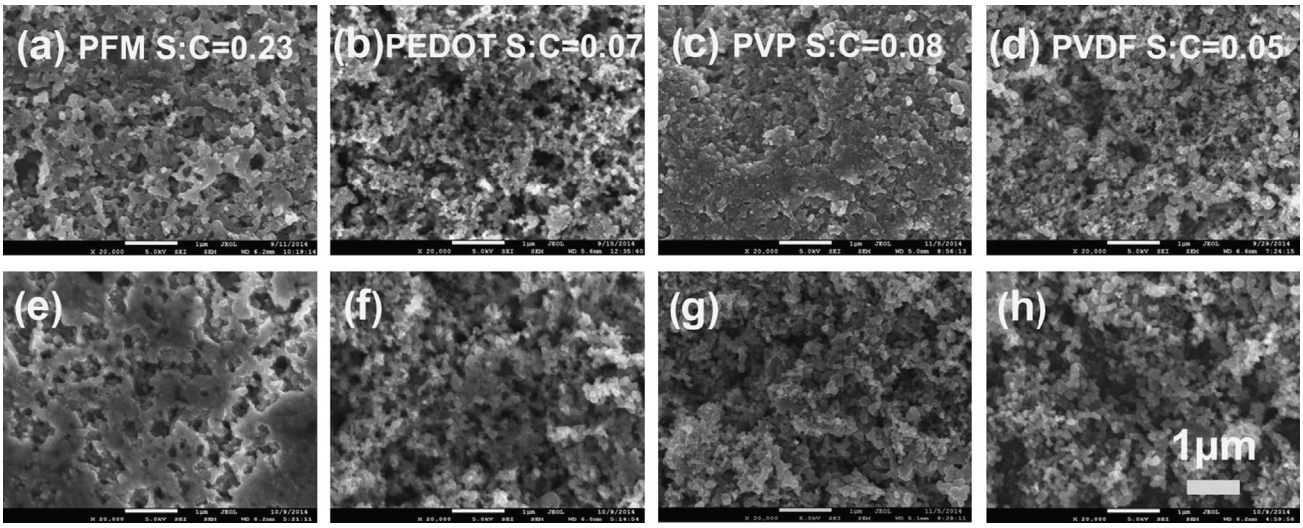

Figure 2 SEM images of the top and bottom morphology of PFM-S (a), (e); PEDOT-S (b), (f); PVP-S(c), (g); PVDF-S (d), (h) in fully charged state. All SEM images have the same magnification in this figure.

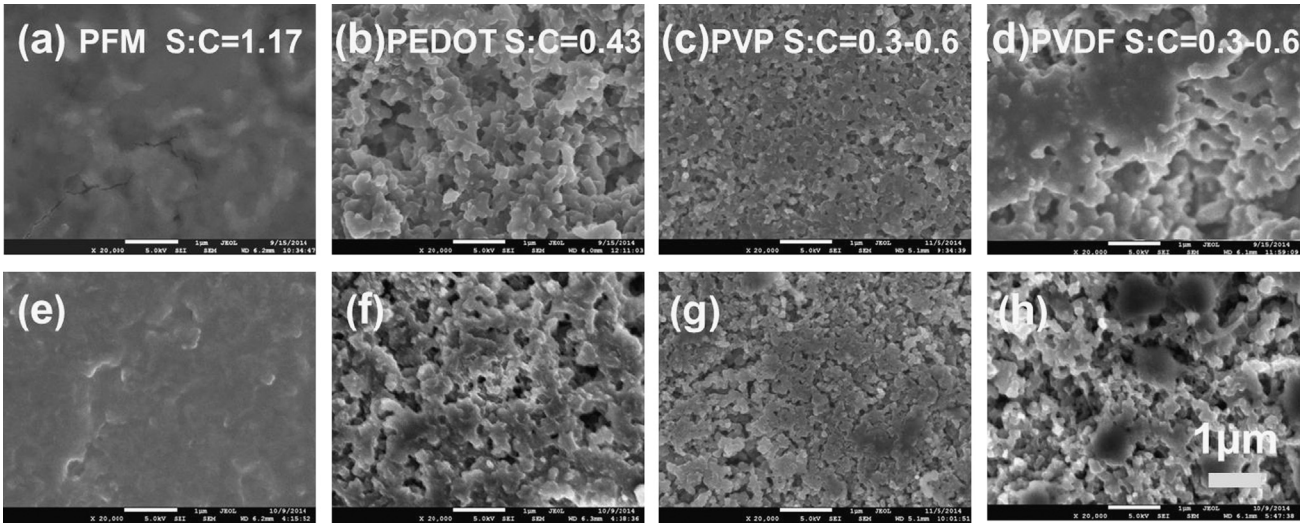

Figure 3 SEM images of the top and bottom morphology of PFM-S (a), (e); PEDOT-S (b), (f); PVP-S(c), (g); and PVDF-S (d), (h) in fully discharged state. All SEM images have the same magnification in this figure.

In fully discharged state, the four cathodes also exhibit differences in SEM morphology. To further observe the solid-phase Li_2S precipitation, the morphology of electrode laminate is observed both from the top surface (Figure 3a–d) and the bottom of the laminate near the current collector (Figure 3e–h). As shown in Figure 3a and e, a large amount of solid-phase Li_2S precipitation is observed for PFM-S; no pore is left void in the film, and the AB layer is totally buried inside. For PEDOT-S (Figure 3b and f), the Li_2S precipitation is a thin solid-phase layer uniformly coated on the surface of AB, indicating good conductivity of PEDOT. But the amount of precipitated Li_2S in PEDOT-S is less than that in PFM-S. In PVP-S in Figure 3c and g, the amount of Li_2S precipitation is a little more than that in PEDOT-S, but less than that in the PFM-S. This results from the strong binding effect of carbonyl group with Li_2S, which can assist Li_2S precipitation. Also, the polar nature of PVP helps to facilitate Li_2S precipitation. But the surface area for Li_2S precipitation is limited by the poor conductivity of PVP, which is also the case in PVDF-S. Li_2S is non-uniformly distributed in PVP-S and PVDF-S (Figure 3d and h). Also, some active material might become isolated from the conductive network and be unable to participate in charge or discharge processes. This loose and non-uniform Li_2S layer can also be identified by the smaller over-potential on the PVDF-S voltage profile compared to that of PFM-S and PEDOT-S at the start of the charge region in Figure 4. This will be discussed in the next section. The sulfur-to-carbon ratio from EDX data is 1.17 for PFM-S, 0.43 for PEDOT-S, and

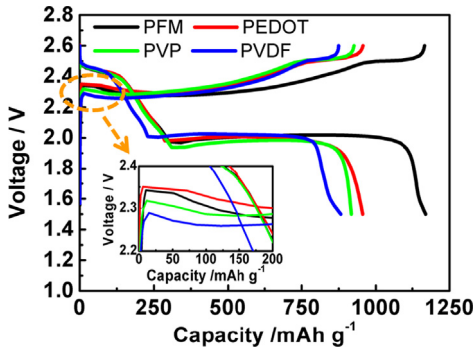

Figure 4 Voltage profile of the tenth cycle of PFM-S, PEDOT-S, PVP-S, and PVDF-S cathodes. Inset shows the detailed voltage curves at the beginning of the charge.

0.3–0.6 (uneven) for PVP-S and PVDF-S, which indicates that far more Li_2S precipitated in PFM-S than in the others.

Surface reaction analysis through charge-discharge voltage profile

The charge–discharge voltage profile at the tenth cycle is used to analyze the detailed phase transformation during charge and discharge processes. As can be observed in Figure 4, the PFM-S, PEDOT-S, and PVP-S show almost the same discharge characteristic in the upper voltage plateau region (2.6–1.95 V), which means the same amount of S_8/Li_2S_8 changed into dissolved state Li_2S_4. However, the voltage profile of the lower voltage plateau region (1.95–1.5 V) is different for these three electrodes: more capacity is obtained in PFM-S than in PEDOT-S and PVP-S. For PFM-S, a capacity of 876 mA h/g is obtained in the lower voltage plateau region, which is 69.7% of the theoretical capacity (1256 mA h/g). However, for PEDOT-S and PVP-S, only 668.5 mA h/g and 606.9 mA h/g capacities are obtained in the lower voltage plateau region, which is 53.2% and 48.3% of the theoretical capacity, respectively. This indicates that the PFM had a positive effect in assisting Li_2S precipitation. Two conclusions can be drawn from this result. First, the strong affinity between the carbonyl functional group of PFM and the sulfur species can assist solid-phase Li_2S precipitation. Second, a much larger conductive surface area of the conductive binder PFM helps to create more reaction sites for Li_2S precipitation. Although the same amount of dissolved state Li_2S_4 is obtained in the upper voltage plateau region, with weaker affinity (PEDOT-S) or less conductive surface area (PVP-S), 30% less Li_2S precipitation is obtained. What is more, in PEDOT-S and PVP-S, there is more residual sulfur species dissolved in the electrolyte, which results in a more severe shuttle effect than with PFM-S. This is the reason that the PEDOT-S and PVP-S showed larger decay than PFM-S during cycling in Figure 1b.

In the fully discharged state, the conductive matrix surface is covered by the solid-phase Li_2S layer. Because of the poor conductivity of the Li_2S layer, only a very limited thickness of Li_2S can precipitate on the conductive surface before the layer turns highly resistive [7]. The characteristic over-potential peak at the beginning of the charge process is closely related to the characteristic of Li_2S layer (Figure 4 inset). Although PVP-S and PVDF-S show a smaller over-potential than PFM-S and PEDOT-S, most of the precipitated Li_2S on PVP-S and PVDF-S nonconductive binder is on the AB. Therefore coating is thinner and inconsistent on the non-functional AB surface. The cathodes do not have large conductive surface to assist Li_2S precipitation where the non-conductive PVP and PVDF partially block the conductive AB surface. So the Li_2S layer is in poor quality and might peel off or isolated from conductive matrix [9,31].

Conclusions

We investigate the effects of both functional group and conductivity of polymer binders on the performance of Li–S batteries. Four different kinds of binders (PFM, PEDOT, PVP, and PVDF) are systematically studied and compared. Both electrochemical performance analysis and post-test analysis are conducted to explore how the polymers influence the electrochemical process through surface reaction effect. The electrodes with different binders show significant differences in the morphology, compositions of sulfur species, and electrochemical characteristics.

PFM, which has the desired functional group and high conductivity, shows the best cycling performance and self-discharge prevention ability among all binders in this work. In both fully charged and discharged states, more solid sulfur species precipitation is observed in cathodes with binders that have carbonyl groups (PFM and PVP) than in cathodes with binders that do not have carbonyl groups (PEDOT and PVDF). This is because the carbonyl group's binding energy with the sulfur species is high, which greatly assists the solid-phase sulfur species precipitation during both the charge and discharge processes. This strong binding effect between the carbonyl group and the sulfur species may help to provide preferred reaction spots for solid-phase product precipitation. The solid-phase sulfur species precipitation will have a positive effect in reducing the shuttle effect, maintaining good self-discharge prevention ability, and achieving long-term cycling stability. The electrical properties of the polymer binders are also important. The conductive binders can help to provide the largest surface area for reactions to take place and effectively assist the resistive solid-phase sulfur species participation in the reactions. In the tests with non-conductive binders, insufficient sulfur species dissolution and non-uniform precipitation are observed.

With a much larger and binding-assisted conductive surface to promote precipitation, PFM-S shows the largest amount of sulfur species precipitation among all the binders studied. These results suggest that both the functional group (the carbonyl group, in this case) and the conductivity of the binder play important roles in assisting the solid-phase sulfur species precipitation (S_8 in charged state and Li_2S in discharged state), which is crucially important in reducing the shuttle effect and achieving good self-discharge and cycling performance in Li–S batteries. Therefore, an improved understanding of how the binder influences the cell performance is necessary and will be helpful for the design of new generation of Li–S binder. Future design of binders for Li–S batteries will need to focus on these issues.

Acknowledgments

This work is funded by the Assistant Secretary for Energy Efficiency, Office of Vehicle Technologies of the U.S. Department of Energy (U.S. DOE) under the Advanced Battery Materials Research (BMR) program, along with the National Center for Electron Microscopy of the Molecular Foundry and the Advanced Light Source at the Lawrence Berkeley National Laboratory, which are supported by the U.S. Department of Energy under Contract DE-AC02-05 CH11231. Junfa Zhu is financial supported from the National Natural Science Foundation of China (U1232102). Guo Ai and Wenfeng Mao are supported by the China Scholarship Council. Jing Yang Wang (University of California, Berkeley) provided the comments and modification on the manuscript.

Appendix A. Supporting information

Supplementary data associated with this article can be found in the online version at http://dx.doi.org/10.1016/j.nanoen.2015.05.036.

References

[1] D. Bresser, S. Passerini, B. Scrosati, Chem. Commun. 49 (2013) 10545–10562.
[2] M. Barghamadi, A. Kapoor, C. Wen, J. Electrochem. Soc. 160 (2013) A1256–A1263.
[3] P.G. Bruce, S.A. Freunberger, L.J. Hardwick, J.-M. Tarascon, Nat. Mater. 11 (2011) 19–29.
[4] X. Ji, S. Evers, R. Black, L.F. Nazar, Nat. Commun. 2 (2011) 325.
[5] Y. Yang, G. Zheng, Y. Cui, Chem. Soc. Rev. 42 (2013) 3018–3032.
[6] M.L. Gordin, F. Dai, S. Chen, T. Xu, J. Song, D. Tang, N. Azimi, Z. Zhang, D. Wang, ACS Appl. Mater. Interfaces 6 (2014) 8006–8010.
[7] Y. Yang, G. Zheng, S. Misra, J. Nelson, M.F. Toney, Y. Cui, J. Am. Chem. Soc. 134 (2012) 15387–15394.
[8] Y.V. Mikhaylik, J.R. Akridge, J. Electrochem. Soc. 151 (2004) A1969–A1976.
[9] S. Evers, T. Yim, L.F. Nazar, J. Phys. Chem. C 116 (2012) 19653–19658.
[10] J. Song, Z. Yu, T. Xu, S. Chen, H. Sohn, M. Regula, D. Wang, J. Mater. Chem. A 2 (2014) 8623–8627.
[11] M. Cuisinier, P.-E. Cabelguen, S. Evers, G. He, M. Kolbeck, A. Garsuch, T. Bolin, M. Balasubramanian, L.F. Nazar, J. Phys. Chem. Lett. 4 (2013) 3227–3232.
[12] J. Song, M.L. Gordin, T. Xu, S. Chen, Z. Yu, H. Sohn, J. Lu, Y. Ren, Y. Duan, D. Wang, Angew. Chem. Int. Ed. Engl. 127 (2015) 1–6.
[13] J. Song, T. Xu, M.L. Gordin, P. Zhu, D. Lv, Y.-B. Jiang, Y. Chen, Y. Duan, D. Wang, Adv. Funct. Mater. 24 (2014) 1243–1250.
[14] G. Zheng, Q. Zhang, J.J. Cha, Y. Yang, W. Li, Z.W. Seh, Y. Cui, Nano Lett. 13 (2013) 1265–1270.
[15] Z.W. Seh, Q. Zhang, W. Li, G. Zheng, H. Yao, Y. Cui, Chem. Sci. 4 (2013) 3673–3677.
[16] H. Yao, G. Zheng, P.-C. Hsu, D. Kong, J.J. Cha, W. Li, Z.W. Seh, M.T. McDowell, K. Yan, Z. Liang, V.K. Narasimhan, Y. Cui, Nat. Commun. 5 (2014) 3943.
[17] J. Song, M. Zhou, R. Yi, T. Xu, M.L. Gordin, D. Tang, Z. Yu, M. Regula, D. Wang, Adv. Funct. Mater. 24 (2014) 5904–5910.
[18] W. Li, Q. Zhang, G. Zheng, Z.W. Seh, H. Yao, Y. Cui, Nano Lett. 13 (2013) 5534–5540.
[19] G. Liu, S. Xun, N. Vukmirovic, X. Song, P. Olalde-Velasco, H. Zheng, V.S. Battaglia, L. Wang, W. Yang, Adv. Mater. 23 (2011) 4679–4683.
[20] M. Wu, X. Xiao, N. Vukmirovic, S. Xun, P.K. Das, X. Song, P. Olalde-Velasco, D. Wang, A.Z. Weber, L.-W. Wang, V.S. Battaglia, W. Yang, G. Liu, J. Am. Chem. Soc. 135 (2013) 12048–12056.
[21] S.-J. Park, H. Zhao, G. Ai, C. Wang, X. Song, N. Yuca, V. S. Battaglia, W. Yang, G. Liu, J. Am. Chem. Soc. 137 (2015) 2565–2571.
[22] H. Zhao, N. Yuca, Z. Zheng, Y. Fu, V.S. Battaglia, G. Abdelbast, K. Zaghib, G. Liu, ACS Appl. Mater. Interfaces 7 (2015) 862–866.
[23] H. Zhao, Z. Wang, P. Lu, M. Jiang, F. Shi, X. Song, Z. Zheng, X. Zhou, Y. Fu, G. Abdelbast, X. Xiao, Z. Liu, V.S. Battaglia, K. Zaghib, G. Liu, Nano Lett. 14 (2014) 6704–6710.
[24] L. Chen, L.L. Shaw, J. Power Sources 267 (2014) 770–783.
[25] Z. Lin, C. Liang, J. Mater. Chem. A 3 (2015) 936–958.
[26] Y. Wang, Y. Huang, W. Wang, C. Huang, Z. Yu, H. Zhang, J. Sun, A. Wang, K. Yuan, Electrochim. Acta 54 (2009) 4062–4066.
[27] M.-K. Song, Y. Zhang, E.J. Cairns, Nano Lett. 13 (2013) 5891–5899.
[28] W. Zhou, X. Xiao, M. Cai, L. Yang, Nano Lett. 14 (2014) 5250–5256.
[29] Z. Wang, Y. Chen, V. Battaglia, G. Liu, J. Mater. Res. 29 (2014) 1027–1033.
[30] M.A. Lowe, J. Gao, H.D. Abruña, RSC Adv. 4 (2014) 18347–18353.
[31] X. Feng, M.-K. Song, W.C. Stolte, D. Gardenghi, D. Zhang, X. Sun, J. Zhu, E.J. Cairns, J. Guo, Phys. Chem. Chem. Phys. 16 (2014) 16931–16940.

Guo Ai is a researcher at China CEPREI Lab, and now is working in Dr. Gao Liu's group as a visiting scholar at Energy Storage and Distributed Resources Division of Lawrence Berkeley National Laboratory. She received her B.S. in Physics at Dalian University of Technology, China in 2007 and her Ph.D. in Physical Electronics in Peking University, China in 2012. Her research interests are electrode design and aging mechanism analysis in lithium-sulfur battery and Li-ion battery.

Yiling Dai is postdoctoral fellow at Energy Storage and Distributed Resources Division of Lawrence Berkeley National Laboratory. He received his B.S. in Applied Chemistry at the Nanjing University, China in 2010 and his Ph. D. in Chemical Engineering at the University of South Carolina-Columbia, USA in 2013. His research focuses on understanding and optimizing electrochemical systems through combination of simulation with experimental work, especially in lithium-sulfur and lithium-ion batteries.

Yifian Ye received his Bachelor's degree from Department of Chemical Physics at University of Science and Technology of China in 2011. He is currently pursuing his Ph. D. under the supervision of Prof. Junfa Zhu at National Synchrotron Radiation Laboratory at University of Science and Technology of China. He is currently a visiting student at Dr. Jinghua Guo's group at Advanced Light Source, Lawrence

Berkeley National Laboratory. His research interests mainly focus on the applications of Synchrotron based probing methods in energy science, such as organic solar cell, organic light-emitting diode and Li–S batteries.

Wenfeng Mao is a Ph.D. candidate in Applied Chemistry in Tianjin University. He is now a visiting student in Dr. Vincent Battaglia's group at Energy Storage and Distributed Resources Division of Lawrence Berkeley National Laboratory. His research mainly focuses on failure analysis and materials synthesis for lithium ion battery.

Zhihui Wang is a senior engineer in Zeptor Corporation of Menlo Park, CA. His work is focused on developing high energy density lithium-ion batteries. Before joining Zeptor, he was a chemist postdoctoral fellow in Environmental Energy Technologies Division of Lawrence Berkeley National Laboratory, working with Dr. Gao Liu on both lithium-ion and lithium-sulfur batteries. He received 1his B.S. and M.S. degrees from Peking University and Ph.D. from State University of New York at Stony Brook.

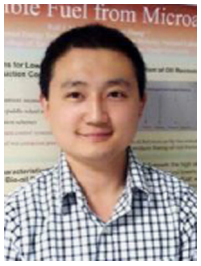

Hui Zhao has been a chemist postdoctoral fellow in Dr. Gao Liu's group at Lawrence Berkeley National Laboratory since 2013. Hui earned his Ph.D. degree in Organic and Polymer Chemistry from Michigan State University in 2012, with a focus on the chemical synthesis and electrochemical performance of polyethylene glycol-based single lithium-ion conductors. His current interests include novel electrolytes and polymer binders for silicon anodes in lithium-ion batteries.

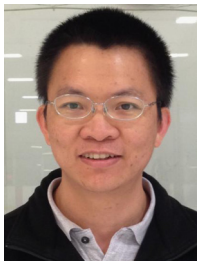

Yulin Chen obtained his bachelor degree in chemistry in 2002 from Nankai University and his master degree in polymer chemistry in 2005 from Guangzhou Institute of Chemistry, Chinese Academy of Sciences. Then he move to United States for graduate research and earned his PhD in organic chemistry in 2012 from University of California, Irvine. He spent one year as a postdoc in Lawrence Berkeley National Lab. Currently, he is a postdoc in Pacific Northwest National Lab. He has expertise on proton exchange membranes, self-healing materials, peptide/peptoid-based biomaterials, conductive binders for lithium ion battery and supramolecular self-assembly.

Junfa Zhu received his Ph.D. in Physical Chemistry from University of Science and Technology of China (USTC) in 1999. After several years working in the Institute of Experimental Physics, Johannes-Kepler-Universität Linz, Austria, Lehrstuhl für Physikalische Chemie II, Friedrich-Alexander-Universität Erlangen-Nürnberg, Germany and Department of Chemistry, University of Washington, WA, USA, he returned to USTC in December, 2006, and become a professor at National Synchrotron Radiation Laboratory, USTC under the support of "Hundred Talent Program" of Chinese Academy of Sciences. His research interests mainly focus on in-situ studies of surface and interface structures and properties of functional materials using advanced surface science techniques.

Yanbao Fu received his M.S. in Chemical Engineering from Qingdao University, and a Ph.D. in Material Science from Fudan University of China. Before coming to LBNL he was an Associate Professor at Fudan University in Department of Materials Science. In 2012 he joined LBNL. Now he is a Staff Research Associate in the Energy Technology Area of LBNL. His current research interests include failure analysis of lithium ion battery, new materials synthesis for lithium ion battery.

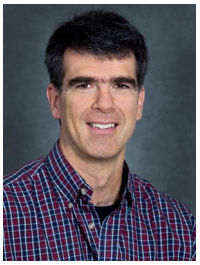

Vince Battaglia heads the Electrochemical Technologies Group at LBNL. Vince has degrees in chemical engineering from The Johns Hopkins University, B.S.; and The University of California at Berkeley, M.S. and Ph.D. Upon graduating he spent 11 years with Argonne National Laboratory's Battery group, with 4(1/2) of those years spent in Illinois and the other 6(1/2) years on assignment in Washington DC as a technical advisor to the Electrochemical Energy Storage Program at D.O.E. His research interests at Lawrence Berkeley National Laboratory are in assessing the energy, power, and cycling limits of advanced battery materials designed for hybrid and electric vehicles.

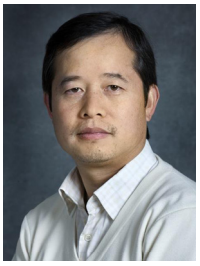

Jinghua Guo is a Senior Scientist at the Advanced Light Source, Lawrence Berkeley National Laboratory, and adjunct professor in the Department of Chemistry and Biochemistry, University of California, Santa Cruz. He received the Ph.D. in Physics at Uppsala University, Sweden, in 1995. He is one of the world's leading experts in the research fields of in-situ/operando soft X-ray spectroscopy. His research interest focuses on the electronic structure, chemical bonding and charge transfer in energy-conversion and energy-storage materials and devices.

Venkat Srinivasan is a Staff Scientist at Lawrence Berkeley National Lab. His research interest is in developing the next-generation batteries for use in vehicle and grid applications. Dr. Srinivasan develops continuum-based models for battery materials and combines them with experimental characterization to help design new materials, electrodes, and devices. His present research focuses on performance and degradation of Li-ion batteries, Mg-ion batteries, and Li–S batteries. Dr. Srinivasan joined the scientific staff at LBNL in 2003 after postdoctoral studies at the University of California, Berkeley and Pennsylvania State University. He received his PhD from the University of South Carolina in 2000.

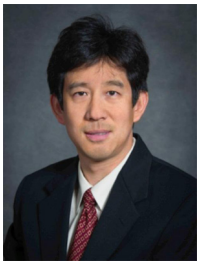

Dr. Gao Liu is a Staff Scientist and Principal Investigator in Energy Technologies Area at Lawrence Berkeley National Laboratory, specialized in lithium battery research. Since he joined Lawrence Berkeley Lab in 2001, Dr. Liu has led energy storage R&D projects for the Department of Energy and industries, and developed key technologies including conductive binders and application of lithium metal to improve battery performance. He has also collaborated with companies to commercialize new battery technologies. He has received numerous awards including R&D100 Award in 2013 and FMC Scientific Achievement Award in 2014.